

On the damage behavior of dielectric films when illuminated with multiple femtosecond laser pulses

Mark Mero

Benjamin Clapp

Jayesh C. Jasapara*

Wolfgang Rudolph

University of New Mexico

Department of Physics and Astronomy

Albuquerque, New Mexico 87131

Detlev Ristau

Kai Starke

Laser Zentrum Hannover e.V.

D-30419 Hannover, Germany

Jörg Krüger

Sven Martin

Wolfgang Kautek†

Federal Institute for Materials Research
and Testing,

D-12200 Berlin, Germany

Abstract. The physical effects reducing the damage threshold of dielectric films when exposed to multiple femtosecond pulses are investigated. The measured temperature increase of a Ta₂O₅ film scales exponentially with the pulse fluence. A polarized luminescence signal is observed that depends quadratically on the pulse fluence and is attributed to two-photon excitation of self-trapped excitons that form after band-to-band excitation. The damage fluence decreases with increasing pulse number, but is independent of the repetition rate from 1 Hz to 1 kHz at a constant pulse number. The repetition rate dependence of the breakdown threshold is also measured for TiO₂, HfO₂, Al₂O₃, and SiO₂ films. A theoretical model is presented that explains these findings. © 2005 Society of Photo-Optical Instrumentation Engineers. [DOI: 10.1117/1.1905343]

Subject terms: laser-induced damage; laser materials; ultrafast phenomena; coatings.

Paper 040564 received Aug. 18, 2004; revised manuscript received Nov. 11, 2004; accepted for publication Dec. 17, 2004; published online May 10, 2005.

1 Introduction

It is well known that the damage threshold fluence of dielectric materials for multipulse exposures is lower compared to single-pulse illumination, an effect that is sometimes called incubation.¹⁻⁵ While this has been observed by many investigators, there is little quantitative systematic study concerning the physical origins of this effect. Optical excitation of dielectric materials can result in the formation of self-trapped excitons (STEs) and subsequently color centers.^{1,6-10} These excitations can be long-lived with lifetimes up to minutes, hours, and even months at room temperature.^{6,10} As such lattice defects can accumulate during multipulse exposure, it is likely that they contribute to the material incubation.

Systematic studies of femtosecond laser-induced damage on oxide dielectric films revealed a dependence of the single-pulse damage fluence $F_{th}(1)$ on pulse duration τ_p and bandgap energy E_g according to

$$F_{th}(1) \approx (c_1 E_g + c_2) \tau_p^\kappa, \quad (1)$$

where $c_1 = 0.074 \pm 0.004 \text{ J cm}^{-2} \text{ fs}^{-\kappa} \text{ eV}^{-1}$, $c_2 = -0.16 \pm 0.02 \text{ J cm}^{-2} \text{ fs}^{-\kappa}$, and $\kappa = 0.30 \pm 0.03$ are material independent constants.^{11(a),(b)} To obtain the critical incident fluence when dealing with thin films, Eq. (1) must be divided by a correction factor that takes into account interference effects.^{11(a)} Equation (1) is explained as the result of the interplay of multiphoton ionization and avalanche ionization. Time-resolved studies of these films showed that a few hundred femtoseconds after excitation, deep defect states

are formed.¹² For Ta₂O₅, for example, the single-pulse incident damage threshold fluence varied from 0.60 J/cm² for $\tau_p = 30 \text{ fs}$ to 1.8 J/cm² for $\tau_p = 1.3 \text{ ps}$.

The damage threshold fluence decreases from the single-shot value $F_{th}(1)$ with pulse number M until a saturated value $F_{th}(\infty)$ is reached.^{2,5,13} Illumination with a fluence $F < F_{th}(\infty)$ does not result in damage regardless of the pulse number M .

In this paper, we present experimental and theoretical results relating to femtosecond-laser-pulse-induced incubation effects in dielectric oxide films. The major results are of general nature and should apply to most dielectric materials, where self-trapped excitons or color centers are known to form as a result of optical excitation.

First, we present measurements of the dependence of the damage threshold on pulse number and repetition rate. The energy deposition into the material is studied by measuring the temperature increase in the film as a function of pulse fluence. The luminescence following excitation is studied as a function of the excitation fluence and provides evidence for the excitation of laser-induced defect states, such as STEs. Finally, we present a phenomenological model that can explain these experimental findings.

2 Experimental Section

All of the experiments were conducted on single-layer films deposited on fused silica substrates. The excitation sources were femtosecond-pulse Ti:sapphire oscillator-amplifier systems operating at a wavelength of 780 and 800 nm with a spatially Gaussian beam profile. The pulse durations varied from 13 to 150 fs.

The measurement of the dependence of the breakdown threshold fluence on repetition rate was performed on TiO₂, Ta₂O₅, HfO₂, Al₂O₃, and SiO₂ films, with an opti-

*Currently at OFS Laboratories, Murray Hill, New Jersey.

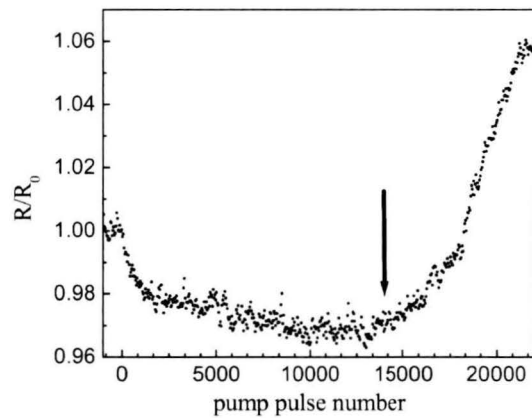
†Currently at the Institute of Physical Chemistry at the University of Vienna, Austria.

Table 1 Sample parameters n_0 , index of refraction at $\lambda=800$ nm; E_g , bandgap energy; and m , order of multiphoton absorption.

Material	n_0	E_g (eV)	m
TiO ₂	2.39	3.3	3
Ta ₂ O ₅	2.17	3.8	3
HfO ₂	2.09	5.1	4
Al ₂ O ₃	1.65	6.5	5
SiO ₂	1.50	8.3	6

cal thickness of $6\lambda/4$ at 790 nm. These materials are commonly used in optical coatings. The films were deposited using ion-beam sputtering (IBS). The samples were illuminated with a burst of 100 pulses ($\tau_p = 30$ fs) at a center wavelength of 800 nm. The material parameters are summarized in Table 1. The technique used to measure the damage threshold fluence was based on the measurement of the ablation crater diameter as a function of the incident pulse energy and extrapolation to a zero-diameter spot to obtain the threshold fluence corresponding to the center of the Gaussian beam.^{5,14}

The measurement of the dependence of the breakdown threshold fluence on pulse number was done on a $6\lambda/4$ Ta₂O₅ film deposited by IBS. The sample was illuminated with 30-fs pulses at a repetition rate of 1 kHz. Depending on the number of laser pulses, two techniques were used to determine the breakdown threshold fluence. For the data points with pulse numbers $M \leq 1000$, the sample was illuminated by bursts containing a certain number of pulses. The increased surface scattering of the laser light at damaged sites is routinely exploited in damage detection.¹⁵ In our experiment, the occurrence of damage was monitored with a CCD camera-microscope detector. This enabled us to monitor the intensity and distribution of light scattered at the excited sample site.¹⁶ A distinct change of the scattered intensity (pattern) of the weak amplified spontaneous emission was visible at the point of surface damage. For illumination we used the (amplified) spontaneous emission (ASE) leaking through the amplifier. In a separate set of experiments, we checked the scattering technique by off-line optical microscopy. For the data points with $M \geq 1000$, we measured the reflectance of the illuminated spot with a weak probe pulse. The probe pulse arrived at the sample approximately 1 ms after the main pulse and thus probed the accumulated reflection change induced by the pulse sequence up to this point. A typical reflection curve as a function of pulse number M for a certain incident fluence is shown in Fig. 1. The reflection gradually decreases with pulse number. At a certain pulse number, the reflection signal increases sharply, which is the point at which damage occurs. Note also that the reflection remains constant at the decreased level if the pump pulse is blocked before damage occurs. In this case, the reflection does not recover on a time scale of several minutes. The experiment was repeated for several fluences, each yielding a certain pulse number at which breakdown was observed. For fluences slightly below $F_{th}(\infty)$, the reflection decrease saturates after a certain number of pulses.

**Fig. 1** Reflection of a weak probe pulse incident <1 ms after the main pulse as a function of the pulse number. The arrow indicates the onset of visible damage.

The damage detection techniques based on the scattering method and the ablation crater diameter analysis were cross-checked and provided¹⁵ identical results within $\pm 10\%$. The damage threshold determined with the scattering method and the technique based on the monitoring of the probe reflection were compared for $M = 1000$ pulses and found to agree within $\pm 5\%$.

The energy deposition into a magnetron-sputtered Ta₂O₅ film was characterized by the induced temperature change. The optical thickness of the film was $10\lambda/4$ at 780 nm. To this end, a sensitive laser calorimeter was built and calibrated.¹⁷ The sample was illuminated with 150-fs pulses centered at 780 nm at a repetition rate of 1 kHz. The pulse fluence was adjusted by changing the laser spot size on the sample while keeping the incident pulse energy (0.2 mJ) constant, with a maximum fluence of 0.4 J/cm^2 , slightly below the breakdown threshold.

To study the luminescence, we focused a 100-MHz repetition rate, 13-fs laser pulse train from the oscillator with a microscope objective onto a $2\lambda/4$ thick Ta₂O₅ IBS film. The luminescence was recorded with a grating spectrometer and a CCD camera.

3 Results

Figure 2 shows the damage threshold as a function of repetition rate for 100 illumination pulses for five different oxide films. The curves show that within experimental error, the multiple-damage threshold does not depend on the repetition rate in the tested region from 1 Hz to 1 kHz. This is in agreement with our observation that the damage threshold depends only on the total number of delivered pulses regardless of the illumination scenario. Identical thresholds were observed for illumination with sequences of bursts of pulses of varying length and duty cycle as long as the total number of pulses was kept constant.

The damage threshold fluence data as a function of pulse number for a Ta₂O₅ film is shown in Fig. 3. The single-shot incident threshold fluence was^{11(a)} $F_{th}(1) \approx 0.6 \text{ J/cm}^2$ at $\tau_p = 30$ fs. The threshold fluence decreases with increasing pulse number and saturates at a value $F_{th}(\infty) \approx 0.67 \times F_{th}(1)$ at $M \approx 1000$. These observations are in agreement with the results of a round-robin experiment done on high-

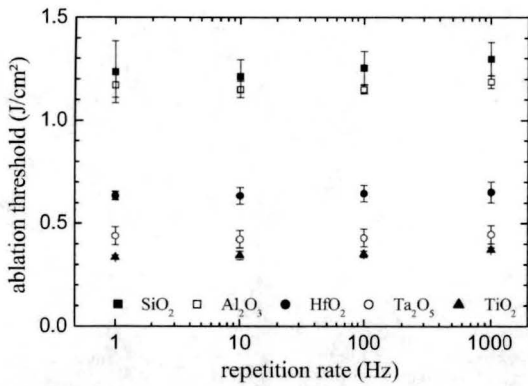


Fig. 2 Incident damage threshold fluence as a function of pulse repetition rate for illumination with $M=100$ pulses and $\tau_p=30$ fs. Results are shown for five different oxide films.

reflection mirrors and antireflection coated windows, where the coatings were made of Ta_2O_5/SiO_2 layers.¹³ In contrast, in multishot experiments² performed on bulk fused silica, CaF_2 , and LiF samples $F_{th}(\infty)$ is reached already at $M < 100$.

The average temperature increase of a Ta_2O_5 film as a function of pulse fluence is shown in Fig. 4. The logarithm of the temperature change increases approximately linearly with the fluence.

The exposure of a Ta_2O_5 film is accompanied by a weak luminescence centered at $\hbar\omega_E \approx 2$ eV. The luminescence polarization is strongly peaked in the direction of the polarization of the excitation pulses. Figure 5 shows the dependence of the luminescence power on the incident pulse intensity. The fit line represents a quadratic dependence of the luminescence power on the laser fluence. Note that the luminescence spectrum does not extend to energies greater than twice the photon energy of the excitation pulse $2\hbar\omega_L$. The maximum fluence used in the experiment was ≈ 0.1

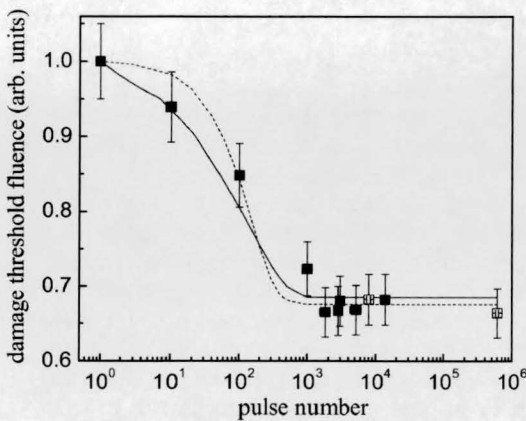


Fig. 3 Damage threshold fluence as a function of the number of illumination pulses. The data represented by the hollow squares were collected under slightly different experimental conditions and were normalized to the other data points. The solid line is the result of simulations using the model based on Eqs. (3) with parameter values given in the text. The dashed line is a fit of the approximate analytical model, cf. Eq. (5). The material was a Ta_2O_5 film deposited on fused silica. The repetition rate was 1 kHz.

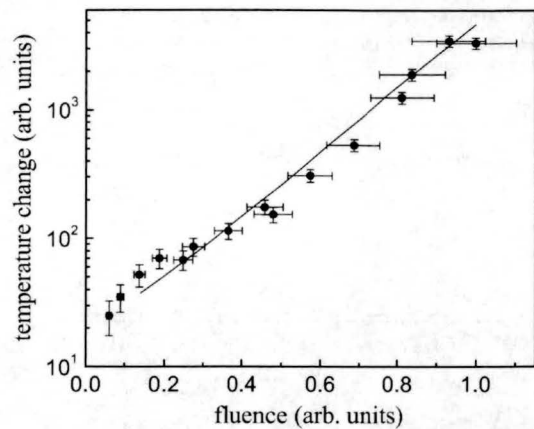


Fig. 4 Average temperature change (log plot) of the Ta_2O_5 film as a function of the incident fluence. The illumination took place with a 1-kHz, 150-fs pulse laser at 800 nm. The solid line is the result of simulations using the model based on Eq. (3) with the same parameter values as in the case of the solid line in Fig. 3.

J/cm^2 , slightly below the breakdown fluence¹⁶ $F_{th}(\infty) = 0.16 J/cm^2$ at $\tau_p = 13$ fs.

4 Discussion and Modeling

Two mechanisms can contribute to the generation of conduction band (CB) electrons—photoionization and electron impact ionization, the latter of which can result in an exponential increase of the number of excited electrons (avalanche ionization) during the excitation. For pulses longer than a few tens of picoseconds, the applicability of the avalanche ionization model to intrinsic, bulk, single-shot laser damage was refuted based on experimental evidence.¹ In the ultrafast pulse domain, the relative contribution of the two effects and their dependence on material and pulse parameters are still debated.^{18–20} A rate equation for the CB electron density was successfully applied to interpret experimental breakdown threshold data in the subpicosecond pulse regime.^{3,11(a),16,18,21,22} Within the framework of this model, the initial energy deposition into Ta_2O_5 at an 800-nm laser center wavelength takes place through a combination of photoionization and avalanche ionization:

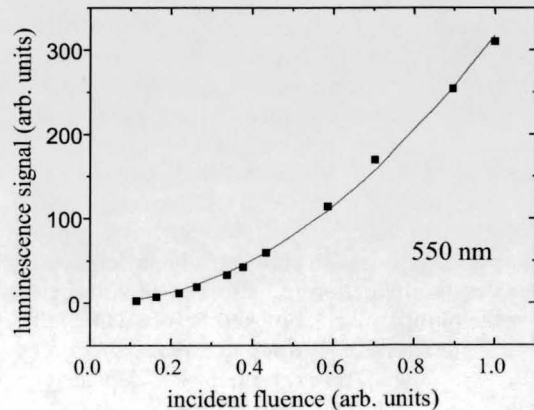


Fig. 5 Luminescence signal at 550 nm from a $\lambda/4$ Ta_2O_5 film as a function of pulse fluence (100 MHz, 13 fs). The solid line represents a fit to a parabola.

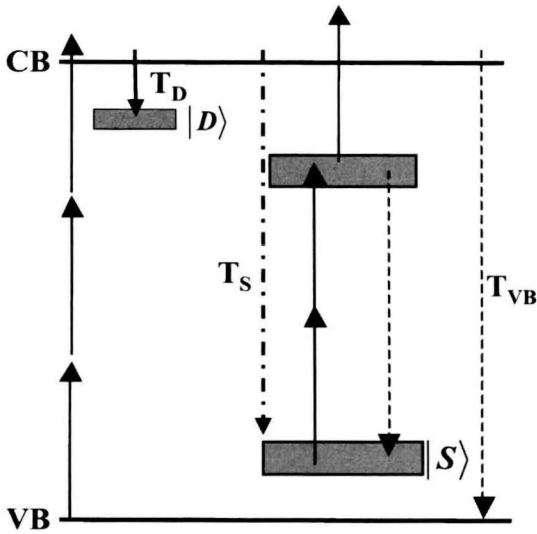


Fig. 6 Energy level diagram of Ta₂O₅: VB, valence band; CB, conduction band; level D, shallow trap; and level S, self-trapped exciton.

$$\frac{dN_{CB}(t)}{dt} = \alpha N_{CB}(t)I(t) + \beta_3 I(t)^3, \quad (2)$$

where $I(t)$ is the laser intensity inside the film, and α and β_3 are the avalanche and the three-photon absorption coefficient, respectively. Damage occurs when a critical electron density^{18,23} is reached in the CB, which is of the order of $N_{CB,cr} = 10^{21} \text{ cm}^{-3}$. This model leads to the pulse duration and bandgap scaling expressed¹¹ in Eq. (1), valid for single-pulse damage. For our simulations, we used $\alpha = 10.5 \text{ cm}^2/\text{J}$ and $\beta_3 = 5.9 \times 10^{24} \text{ cm}^3 \text{ fs}^2/\text{J}^3$, which were obtained from single-shot breakdown threshold fluence data recorded as a function of pulse duration.^{11(a)}

Our modeling is based on the energy diagram sketched in Fig. 6. Once in the conduction band, electrons can relax to the valence band (VB) with a characteristic time constant T_{VB} or decay into shallow traps (D) and STEs (S) with time constants T_D and T_S , respectively. The latter processes are assumed to follow bimolecular decay laws. The density of self-trapped excitons saturates at a certain value $N_{S,max}$. STEs are well-known lattice defects observed in many wide-gap dielectric materials. Time-resolved pump probe measurements have shown that defects, possibly STEs, with a binding energy larger than the single photon energy at 800 nm (1.55 eV) form a few hundred femtoseconds after excitation in TiO₂, Ta₂O₅, and HfO₂ films.¹² These STEs are long-lived and can accumulate during illumination by a sequence of pulses. Shallow traps are typical for coatings and manifest themselves as small tails in the transmission spectrum near the bandgap observed in our oxide films.

The quadratic fluence dependence of the luminescence signal shown in Fig. 5 and the cutoff of the spectrum at $2\hbar\omega_L$ suggest that the STEs can be excited by the near-IR (NIR) femtosecond pulses through two-photon absorption. STE luminescence is known to be polarized due to the well-defined transition dipoles associated with the corresponding electron-hole recombination.²⁴ As the structure of

our investigated films is nearly amorphous, the STE absorption and fluorescence behavior is controlled by dipole moments that are randomly oriented. However, excitation with a linearly polarized laser is expected to result in a polarized luminescence that peaks along an axis that is parallel to the laser polarization.

Figure 6 shows the simplest energy diagram that is in accord with the experiments. The double-level structure in the forbidden gap can explain a defect binding energy in excess of 1.55 eV, the two-photon STE recombination luminescence, and the fact that the self-trapping process occurs through non-radiative processes at room temperature.

The electron density in the CB is described by the following set of rate equations:

$$\begin{aligned} \frac{dN_{CB}(t)}{dt} &= \alpha N_{CB}(t)I(t) + \beta_3 I(t)^3 + \sigma_S N_S(t)I(t)^3 \\ &+ \sigma_D N_D(t)I(t) - \frac{N_{CB}(t)}{T_D} \left(1 - \frac{N_D(t)}{N_{D,max}}\right) \\ &- \frac{N_{CB}(t)}{T_S} \left(1 - \frac{N_S(t)}{N_{S,max}}\right) - \frac{N_{CB}(t)}{T_{VB}}, \\ \frac{dN_S(t)}{dt} &= -\sigma_S N_S(t)I(t)^3 + \frac{N_{CB}(t)}{T_S} \left(1 - \frac{N_S(t)}{N_{S,max}}\right), \\ \frac{dN_D(t)}{dt} &= -\sigma_D N_D(t)I(t) + \frac{N_{CB}(t)}{T_D} \left(1 - \frac{N_D(t)}{N_{D,max}}\right), \end{aligned} \quad (3)$$

where N_D and N_S are the number densities of shallow traps and ground-state STEs, respectively; $N_{D,max}$ and $N_{S,max}$ are the maximum shallow trap and STE densities, respectively; and the quantities $3\hbar\omega_L\sigma_S$ and $\hbar\omega_L\sigma_D$ are the three- and one-photon absorption cross sections of the STEs and the shallow trap states, respectively. We neglected the effects of the weak luminescence on the occupation numbers. The two-step resonant ionization of the ground state STEs was approximated with a three-photon absorption process.

The production of seed electrons in the CB that start the avalanche process can proceed via three channels—(1) multiphoton ionization from the VB, (2) two-photon absorption by the STE followed by a one-photon ionization (lumped into a three-photon ionization), and (3) one-photon ionization of shallow traps. Avalanche ionization acts then on these seed electrons and can lead to a significant increase in N_{CB} . Because of a resonant intermediate level, the rate of CB electron production through channel 2 can be comparable to that of channel 1 if a certain STE density is reached. Thus, the damage threshold is expected to decrease with pulse number. Saturation of the exciton density is responsible for the saturation of the damage threshold at large pulse numbers. If $N_{D,max} \ll N_{cr}$, the ionization of shallow traps has a significant effect (relative to channels 1 and 2) on the CB seed electron production only at low fluences.

Simulations based on Eqs. (3) were performed to reproduce $F_{th}(M)$ and the fluence dependent temperature behavior simultaneously. The quantities σ_S and $N_{S,max}$ were adjusted to match the pulse number, where the threshold fluence saturates, and the ratio $F_{th}(\infty)/F_{th}(1)$. To explain

the temperature increase ΔT of the film and its dependence on the incident fluence we assume that a steady state has been reached, where the CB excitation produced by one pulse completely relaxes before the next pulse arrives. We further assume that the temperature increase is proportional to the number of electrons excited to the CB by one excitation pulse, which represents the total energy deposition into the material. We adjusted $N_{D,\max}$ to reproduce the approximate linearity of the $\log(\Delta T)$ versus F dependence, where the σ_D value was set such that all of the shallow traps are ionized by each consecutive pulse for our experimental fluence regime. If $N_{D,\max}$ is too small, the $\log(\Delta T)$ versus F curve deviates from a straight line at low fluences, resulting in ΔT values smaller than what was observed experimentally. We adjusted T_{VB} relative to a preset T_S . The simulation results were normalized to the experimental data. Since the breakdown threshold is independent of repetition rate from 1 Hz to 1 kHz, we can conclude that the relaxation times T_D , T_S , and T_{VB} are much shorter than 1 ms.

The result of the simulation is shown by the solid lines in Figs. 3 and 4, obtained with $T_D=200$ fs, $T_S=1$ ps, $T_{VB}=1.1$ ps, $\sigma_D=500$ cm²/J, $\sigma_S=390$ cm⁶ fs²/J³, $N_{D,\max}=5\times 10^{18}$ cm⁻³, and $N_{S,\max}=10^{23}$ cm⁻³. With this set of parameter values, the model can explain the most important features of the experimental data. However, the extracted value for the upper limit of the STE density $N_{S,\max}$ seems to be too large, while T_{VB} is too small. The reason why a large $N_{S,\max}$ value is predicted by the model can be understood as follows. Saturation of the decrease of F_{th} occurs when the maximum defect density is reached. Due to the fast creation of STEs, a large number of electrons are trapped after each pulse. Therefore, an $N_{S,\max}$ much larger than the CB electron density produced by one pulse is necessary to allow for a slow, gradual decrease of F_{th} with M . With a much larger T_{VB} (i.e., $T_{VB}/T_S \gg 1$), $N_{S,\max}$ increases to just a few times 10^{23} cm⁻³. The introduction of a transient state in the model that decays into a final metastable state (STE or color center) with low efficiency would lead to a lower maximum defect density value. The exact physical origin of such an intermediate and final state in Ta₂O₅ is not clear at this point. For SiO₂ and CaF₂, however, formation of different types of color centers by photoexcitation of hole and electron self-trapped states was observed.^{24,25} A lower value for the critical electron density, $N_{CB,cr}$ would also result in a lower maximum defect density.

The ionization of shallow traps with a density of approximately 10^{18} cm⁻³ makes sure that the linearity of the $\log(N_{CB})$ versus F curve is maintained not only at high, but at low fluences as well. However, the existence of shallow traps does not affect the breakdown threshold as direct band-to-band excitation and STE ionization dominate the CB electron production at high fluences.

The approximately linear behavior of the $\log(\Delta T)$ versus F curve can also be understood based on Eq. (2), if we add the effect of shallow traps and STEs. Under steady state conditions, the ionization of STEs can be lumped into a constant effective three-photon absorption coefficient, so that β_3 in Eq. (2) can be replaced by $\beta_{3,\text{eff}}=\beta_3+\sigma_S N_{S,\max}$. If σ_D is large enough, the shallow defects are fully ionized

by the leading edge of each laser pulse through one-photon absorption even at low fluences. In the steady state, this leads to a constant contribution to N_{CB} . Therefore, the electron density trapped in the shallow defects can be considered as a ‘‘background’’ CB electron density with a value equal to $N_{D,\max}$, which does not relax between consecutive laser pulses. With these assumptions, Eq. (2) was solved analytically for N_{CB} assuming pulses with a square-shaped temporal profile. We obtain for the CB electron density excited by one pulse, which is proportional to the temperature increase:

$$N_{CB}=N_{D,\max} \exp(\alpha F) \left\{ 1 + \frac{N^*}{N_{D,\max}} \left[1 - \frac{1}{\exp(\alpha F)} \right] \right\}, \quad (4)$$

where the parameter $N^*=\beta_{3,\text{eff}}F^2/(\alpha\tau_p^2)$. If the laser beam has a spatial profile, F describes the fluence at a certain location within the beam, for example, at the beam center. The limits of N_{CB} in the low- and high-fluence regimes are $N_{D,\max} \exp(\alpha F)$ and $N_{D,\max} \exp(\alpha F)N^*/N_{D,\max}$, respectively. On a logarithmic scale, the leading term in both cases, $F\alpha \log(e)$, is linear in F . Note that without the background electron density (shallow trap states) and/or without the avalanche ionization term the linear behavior of $\log(N_{CB})$ versus F cannot be reproduced.

We note that replacing the bi-molecular term describing the CB electron trapping into state S in Eq. (3) by a mono-molecular term leads to qualitatively similar results. However, the assumption of a maximum possible STE density is still necessary in order to obtain the saturation behavior of the damage threshold fluence as a function of pulse number.

To explore the parameter dependencies of the model expressed by Eqs. (3) and to suggest a practicable fit function to multiple pulse damage data we attempted an approximate analytical solution. As explained earlier, for fluences near the critical fluence we can neglect the effect of the shallow traps. With the simplifying assumption that in the absence of STEs each (temporally square shaped) pulse excites N_C electrons to the conduction band that relax completely either into STEs or back to the VB before the next pulse arrives, we can calculate the number of STEs after $M-1$ pulses.²⁶ The next excitation pulse produces a CB electron density $N_{CB}(M) \approx F^3\beta_3G\tau_p^{-2}\{1+\sigma'N_{S,\max}[1-(1-T_{VB}B/T_S)^{M-1}]\}$, where $\sigma'=\sigma_S/\beta_3$, $B=N_C/N_{S,\max}$, and G is the electron multiplication factor due to avalanche ionization that is assumed to be independent of the laser fluence. Damage occurs at a pulse number M' for which $N_{CB}(M')=N_{cr}$. This leads to a damage fluence as function of pulse number:

$$F_{th}^3(M) = F_{th}^3(\infty) + [F_{th}^3(1) - F_{th}^3(\infty)] \left(1 - \frac{T_{VB}}{T_S} B \right)^{M-1}, \quad (5)$$

where $F_{th}^3(1)=N_{cr}\tau_p^2/(\beta_3G)$ and $F_{th}^3(\infty)=F_{th}^3(1)/(1+\sigma'N_{S,\max})$. The dashed line in Fig. 3 shows the graph according to $F_{th}(\infty)/F_{th}(1)=0.675$ obtained from the data, and a best fit value for $(1-BT_{VB}/T_S)=0.991$. A value $BT_{VB}/T_S \ll 1$ is in agreement with $N_{S,\max} \gg N_C$ predicted by

the numerical model based on Eqs. (3). The parameter values used in the numerical model yield $BT_{VB}/T_S = 3 \times 10^{-4}$.

5 Summary

Femtosecond-laser-pulse-induced incubation effects in Ta_2O_5 films were investigated experimentally and theoretically. In addition, the repetition rate dependence of the breakdown threshold fluence was also measured for TiO_2 , HfO_2 , Al_2O_3 , and SiO_2 films. The observed incubation behavior of Ta_2O_5 shows similarities to the incubation behavior of TiO_2 , HfO_2 (Ref. 12), and SiO_2 (Ref. 24). These results suggest that the conclusions of our experiments on Ta_2O_5 are also applicable to other dielectric materials.

The decrease of the damage threshold with the pulse number was explained with the accumulation and ionization of self-trapped excitons. The formation of these excitons occurs on a time scale much faster than 1 ms and the lifetime of these defects exceeds tens of minutes. This explains the observation that the damage threshold is independent of the repetition rate from 1 Hz to 1 kHz. Resonant excitation of the excitons results in a weak luminescence whose quadratic dependence on the excitation fluence is characteristic for a two-photon absorption. A rate equation model for the CB electron density that includes STEs and shallow traps was solved to explain the multiple-pulse damage behavior. This model was also successfully applied to reproduce the measured temperature increase of the film and its dependence on the excitation fluence. According to the model, the STEs control the dependence of the damage threshold fluence on the pulse number, while the shallow traps are necessary to reproduce the observed temperature increase at low fluences.

Acknowledgments

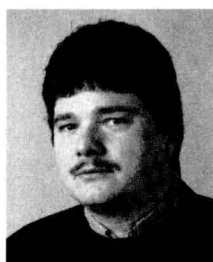
The authors thank Dr. J. Liu for helpful discussions and support with the data acquisition. The project was supported by the National Science Foundation (NSF) under Grant No. ECS-0100636 and Grant No. DGE-0114319 and by the Defense Advanced Research Projects Agency–Joint Technology Office (DARPA-JTO) under Grant No. 2001-025. The Berlin group acknowledges financial support by the German Federal Ministry of Education and Research in the framework of the project “Safety for Applications of Femtosecond Laser Technology”—SAFEST (BMBF-Projektverband Femtosekundentechnologie).

References

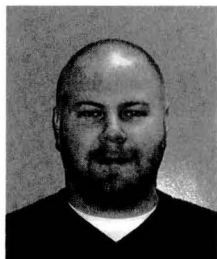
1. S. C. Jones, P. Braunlich, R. T. Casper, X.-A. Shen, and P. Kelly, “Recent progress on laser-induced modifications and intrinsic bulk damage of wide-gap optical materials,” *Opt. Eng.* **28**, 1039–1068 (1989).
2. A. Rosenfeld, M. Lorenz, R. Stoian, and D. Ashkenasi, “Ultrashort-laser-pulse damage threshold of transparent materials and the role of incubation,” *Appl. Phys. A: Mater. Sci. Process.* **69**, S373–S376 (1999).
3. A.-C. Tien, S. Backus, H. Kapteyn, M. Murnane, and G. Mourou, “Short-pulse laser damage in transparent materials as a function of pulse duration,” *Phys. Rev. Lett.* **82**, 3883–3886 (1999).
4. G. J. Exarhos, A. H. Guenther, N. Kaiser, M. R. Kozlowski, K. L. Lewis, M. J. Soileau, and C. J. Stolz, Eds., *Proceedings of the Laser-Induced Damage in Optical Materials, Collected Papers, Boulder, 1999–2003*, SPIE, Bellingham, WA (2004).
5. J. Bonse, J. M. Wrobel, J. Krüger, and W. Kautek, “Ultrashort-pulse laser ablation of indium phosphide in air,” *Appl. Phys. A: Mater. Sci. Process.* **72**, 89–94 (2001).
6. R. T. Williams, “Optically generated lattice defects in halide crystals,” *Opt. Eng.* **28**, 1024–1033 (1989); N. Itoh and K. Tanimura, “Effects of photoexcitation of self-trapped excitons in insulators,” *Opt. Eng.* **28**, 1034–1038 (1989).
7. S. Guizard, P. Martin, G. Petite, P. D’Oliveira, and P. Meynadier, “Time-resolved study of laser-induced colour centres in SiO_2 ,” *J. Phys.: Condens. Matter* **8**, 1281–1290 (1996).
8. Ch. Görling, U. Leinhos, and K. Mann, “Self-trapped exciton luminescence and repetition rate dependence of two-photon absorption in CaF_2 at 193 nm,” *Opt. Commun.* **216**, 369–378 (2003).
9. J. B. Lonzaga, S. M. Avanesyan, S. C. Langford, and J. T. Dickinson, “Color center formation in soda-lime glass with femtosecond laser pulses,” *J. Appl. Phys.* **94**, 4332–4340 (2003).
10. A. Hertwig, S. Martin, J. Krüger, and W. Kautek, “Surface damage and color centers generated by femtosecond pulses in borosilicate glass and silica,” *Appl. Phys. A: Mater. Sci. Process.* **79**, 1075–1077 (2004).
11. (a) M. Mero, J. Liu, W. Rudolph, D. Ristau, and K. Starke, “Scaling laws of femtosecond laser pulse induced breakdown in oxide films,” *Phys. Rev. B* **71**, 115109 (2005); (b) J. Jasapara, M. Mero, and W. Rudolph, “Retrieval of the dielectric function of thin films from femtosecond pump-probe experiments,” *Appl. Phys. Lett.* **80**, 2637–2639 (2002).
12. M. Mero, A. J. Sabbah, J. Zeller, and W. Rudolph, “Femtosecond dynamics of dielectric films in the pre-ablation regime,” *Appl. Phys. A: Mater. Sci. Process, Online First* (8 pages) (2005).
13. K. Starke, D. Ristau, S. Martin, A. Hertwig et al., “Results of a round-robin experiment in multiple-pulse LIDT measurement with ultrashort pulses,” *Proc. SPIE* **5273**, 388–395 (2003).
14. J. M. Liu, “Simple technique for measurement of pulsed Gaussian-beam spot sizes,” *Opt. Lett.* **7**, 196–198 (1982).
15. J. Bonse, S. Baudach, J. Krüger, W. Kautek, K. Starke, T. Groß, D. Ristau, W. Rudolph, J. Jasapara, and E. Welsch, “Femtosecond laser damage in dielectric coatings,” *Proc. SPIE* **4347**, 24–34 (2001).
16. J. Jasapara, A. V. V. Nampoothiri, W. Rudolph, D. Ristau, and K. Starke, “Femtosecond laser pulse induced breakdown in dielectric thin films,” *Phys. Rev. B* **63**, 045117 (2001).
17. K. Starke, D. Ristau, and H. Welling, “Standard measurement procedures for the characterization of fs-laser optical components,” *Proc. SPIE* **4932**, 482–491 (2002).
18. B. C. Stuart, M. D. Feit, S. Herman, A. M. Rubenchik, B. W. Shore, and M. D. Perry, “Nanosecond-to-femtosecond laser-induced breakdown in dielectrics,” *Phys. Rev. B* **53**, 1749–1761 (1996).
19. A. Kaiser, B. Rethfeld, M. Vicanek, and G. Simon, “Microscopic processes in dielectrics under irradiation by subpicosecond laser pulses,” *Phys. Rev. B* **61**, 11437–11450 (2000); B. Rethfeld, “Timescales in the response of materials to femtosecond laser excitation,” *Phys. Rev. Lett.* **92**, 187401 (2004).
20. F. Quere, S. Guizard, Ph. Martin, G. Petite, H. Merdji, B. Carre, J.-F. Hergott, and L. Le Deroff, “Hot-electron relaxation in quartz using high-order harmonics,” *Phys. Rev. B* **61**, 9883–9886 (2000); F. Quere, S. Guizard, and Ph. Martin, “Time-resolved study of laser-induced breakdown in dielectrics,” *Europhys. Lett.* **56**, 138–144 (2001).
21. M. Lenzner, J. Krüger, S. Sartania, Z. Cheng, Ch. Spielmann, G. Mourou, W. Kautek, and F. Krausz, “Femtosecond optical breakdown in dielectrics,” *Phys. Rev. Lett.* **80**, 4076–4079 (1998).
22. C. B. Schaffer, A. Brodeur, and E. Mazur, “Laser-induced breakdown and damage in bulk transparent materials induced by tightly focused femtosecond laser pulses,” *Meas. Sci. Technol.* **12**, 1784–1794 (2001).
23. D. Du, X. Liu, G. Korn, J. Squier, and G. Mourou, “Laser-induced breakdown by impact ionization in SiO_2 with pulse widths from 7 ns to 150 fs,” *Appl. Phys. Lett.* **64**, 3071–3073 (1994).
24. C. Itoh, K. Tanimura, and N. Itoh, “Optical studies of self-trapped excitons in SiO_2 ,” *J. Phys. C* **21**, 4693–4702 (1988).
25. K. Tanimura, T. Katoh, and N. Itoh, “Lattice relaxation of highly excited self-trapped excitons in CaF_2 ,” *Phys. Rev. B* **40**, 1282–1287 (1989).
26. M. Mero, “Femtosecond laser induced electron-lattice dynamics and breakdown of dielectric optical coatings,” Ph.D. thesis, University of New Mexico (2005).



Mark Mero received his diploma in physics from the University of Szeged, Hungary, in 1998 and he is currently working toward his PhD degree in optical sciences and engineering at the University of New Mexico in the field of high-intensity laser/matter interaction. His research interests include ultrashort laser pulse characterization, femtosecond pump-probe spectroscopy, and femtosecond-laser-pulse-induced ablation and modification of dielectric materials.



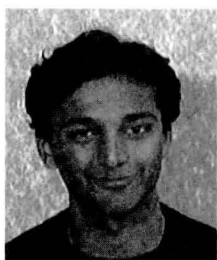
Jörg Krüger received his physics diploma degree and his Dr Rer Nat degree from the University of Jena, Germany, and the Brandenburg University of Technology Cottbus, Germany. Since 1991, he has been with the Federal Institute for Materials Research and Testing (BAM) in Berlin, Germany. He currently heads a working group dealing with ultra-short-pulse laser technology.



Benjamin Clapp received his BS degree from Purdue University, Fort Wayne, Indiana, in 2002, and he is currently a PhD student in optical sciences and engineering at the University of New Mexico. His doctoral research focuses on thin film studies and high-contrast microscopy; each utilizes femtosecond laser sources.



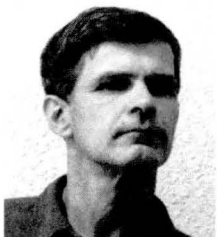
Sven Martin received his physics diploma degree from the University of Jena, Germany. In 2001 he joined the working group for ultra-short-pulse laser technology at the Federal Institute for Materials Research and Testing (BAM) in Berlin, Germany.



Jayesh C. Jasapara earned his undergraduate degree in engineering physics from the Indian Institute of Technology, Bombay, in 1995. His graduate work on the breakdown of optical thin films under femtosecond-pulse illumination earned him a PhD degree in optical sciences from the University of New Mexico in 2001. He then joined Bell Labs, where he investigated the dispersion properties of photonic bandgap fibers. He is currently with OFS Labs. His interests include optical coherence tomography (OCT), supercontinuum generation, ultrafast carrier dynamics in wideband dielectrics, and high-power fiber lasers.



Wolfgang Kautek received his diploma in chemical engineering in 1976 from the Vienna University of Technology, Austria, and his doctoral degree in 1980 from the University of Technology, Berlin, Germany. From 1976 to 1987 he was a research scientist with the University of Kentucky, USA, at the Fritz-Haber-Institute of the Max-Planck-Society, Berlin, at the IBM San Jose Research Laboratory, California, USA, and the Siemens Research Center, Erlangen, Germany. In 1981 he was awarded the Otto-Hahn-Medal of the Max-Planck-Society and was a visiting professor with the Department of Physics of the Simon-Fraser-University, Burnaby, Vancouver, British Columbia, Canada. He headed the Laboratory for Thin Film Technology of the Federal Institute for Materials Research and Testing, Berlin, from 1988 to 2004. He became a lecturer at the Institute for Physical Chemistry of the Free University Berlin, Germany, in 1994, an adjunct professor at the Institute of Chemistry of the Free University Berlin, Germany, in March 2003, and full professor of physical chemistry at the University of Vienna in 2004. He has more than 200 open literature publications, holds four patents, and has given over 350 presentations, of which more than 180 were invited. His research interests are laser electrochemistry, electrochemical *in situ* techniques, and materials processing with subpicosecond lasers.



Wolfgang Rudolph received his diploma in physics in 1982 and his PhD degree in physics in 1985 from the Friedrich-Schiller-University, Jena. In 1991 he joined the faculty of the Department of Physics and Astronomy of the University of New Mexico (UNM) in Albuquerque where he is a professor of physics and electrical engineering. He coauthored two books—*Ultrashort Light Pulse Compression* (Harwood Academic Publishers, London, 1989) and *Ultrashort Laser Pulse Phenomena* (Academic Press, New York, 1996). His research interests include ultrashort laser pulses and spectroscopy, microscopic imaging, and IR lasers. He chaired the Optics Program at UNM and is currently the associate chair of the Physics Department.



Detlev Ristau has been active in the field of optical thin film technology since 1982. He received his PhD degree from the University of Hannover in 1988. Currently, he is leading the Department of Thin Film Technology at the Laser Zentrum Hannover. Dr. Ristau is the author or coauthor of more than 150 publications concentrating on the production and characterization of coatings for applications in laser technology and optics.

Kai Starke: Biography and photograph not available.